Industrial Research Limited Report 1110

Calibration uncertainty for a 3-sampler vector network analyser

B. D. Hall

Measurement Standards Laboratory of New Zealand
Lower Hutt, New Zealand

1 December 2006 (Replaces versions: 26 February 2004 and 19 July 2002)

Calibration uncertainty for a 3-sampler vector network analyser

B. D. Hall

Industrial Research Limited Report 1110

Reference

B. D. Hall; 1 December 2006 (Replaces versions: 26 February 2004 and 19 July 2002). Calibration uncertainty for a 3-sampler vector network analyser. Industrial Research Limited Report 1110; Lower Hutt, New Zealand.

Summary

This report addresses the question of assessing the measurement uncertainty in a set of correction terms obtained for a vector network analyser (VNA) by a standard calibration procedure (the OSLT – open-short-load-thru – procedure).

The report collects together material from diverse sources to provide a useful resource for developing measurement applications that incorporate VNA measurements. To our knowledge, a complete mathematical description of this problem has not been given in full, so this report represents a valuable reference with regard to calculating calibration uncertainty for VNAs.

The report contains:

- A review of the relevant concepts in uncertainty and uncertainty propagation in the case of bivariate (complex-valued) quantities;
- The equations relating to the OSLT procedure, with some explanations;
- The equations describing the uncertainty in the derived correction terms;
- A numerical application.

Contents

1 Change history

1.1 Changes in the third version

Several equation term errors have been corrected:

- Equation (29), $E_{\mathrm{R}}^{\mathrm{R}}$ changed to $E_{\mathrm{R}}^{\mathrm{F}}$ in the second term in the numerator
- Equation (33), S_{22}^{R} changed to S_{11}^{R} in the denominator
- Equation (35), S_{22}^{R} changed to S_{11}^{R} in the denominator

1.2 Changes in the second version of this report

After about a year of good use, it was clear that to preserve a growing number of pencil annotations to the 'working copy' of this report, the electronic copy should be revised. Nothing has been removed or changed from the previous version (with the exception of one correction to an equation). The report has been extended with a few more equations and a complex expression for some of the equations, which is considerably more convenient to handle. Section numbering has changed as a consequence of the additions.

The changes to the report of 19 July 2002 are as follows:

- Subsection 3.3 has been added, describing the relationship of complex derivatives to bivariate Jacobian matrices.
- Subsection 4.1 has been added describing the error correction model for one port of a VNA.
- The sign of equation (33) was wrong and has been corrected (NB, the error was imported from [5]).
- Throughout Section 5, complex equivalents of equations have been added to supplement the scalar forms. In particular, Section 5.1.1 has been added, detailing the form of the one-port uncertainty matrix calculations in complex number format.

2 Uncertainty in complex quantities

This section reviews some well-known statistical results and methods that apply to bivariate data.

2.1 Bivariate sample statistics

For measurement uncertainty calculations the *sample mean* and the *variance-covariance of the sample mean* are of principal interest. The mean of n values $\mathbf{x}_j \equiv [x_{1j}, x_{2j}]'$, where $j = 1, \cdots, n$, is

$$\mathbf{z} = \begin{bmatrix} z_1 \\ z_2 \end{bmatrix} , \tag{1}$$

where the components are

$$z_i = \frac{1}{n} \sum_{j=1}^{n} x_{ij} \tag{2}$$

The 2×2 sample estimate of the variance-covariance matrix of the sample mean is

$$\mathbf{V_z} = \begin{bmatrix} v_{11} & v_{12} \\ v_{21} & v_{22} \end{bmatrix} , \tag{3}$$

with elements

$$v_{ik} = \frac{1}{n(n-1)} \sum_{j=1}^{n} (x_{ij} - z_i)(x_{kj} - z_k) \ . \tag{4}$$

Appealing to the central limit theorem, the sampling distribution of the sample-mean is approximately normal (exactly so, if the population is normal too). If the variance-covariance of the *population* is $\mathbf{\Sigma}$ then the variance-covariance of the distribution of the *sample mean* will be $\mathbf{\Sigma}/n$.

2.2 The bivariate normal distribution

The bivariate normal density function can be expressed as a function of $\mathbf{x}$ with parameters μ, the mean, and $\mathbf{\Sigma}$, the population variance-covariance as:

$$f(\mathbf{x}) = \frac{1}{2\pi|\mathbf{\Sigma}|^{1/2}} \exp\left[-\frac{1}{2}(\mathbf{x} - \boldsymbol{\mu})' \mathbf{\Sigma}^{-1} (\mathbf{x} - \boldsymbol{\mu}) \right] \ . \tag{5}$$

A contour of constant density is an ellipse centred on $\boldsymbol{\mu}$ of the form

$$c^2 = (\mathbf{x} - \boldsymbol{\mu})' \mathbf{\Sigma}^{-1} (\mathbf{x} - \boldsymbol{\mu}) \ . \tag{6}$$

The axes of the ellipse are $\pm c\sqrt{\lambda_i}\mathbf{e}_i$, where $(\lambda_i, \mathbf{e}_i)$ is an eigenvalue-eigenvector pair of $\mathbf{\Sigma}$.

2.3 Bivariate confidence region for the mean

A contour of constant density can determine the boundary of a confidence region for the mean of a bivariate normal distribution. For a distribution of *known* covariance $\mathbf{\Sigma}$, and for a sample-mean vector $\mathbf{z}$ obtained from a sample of size n, the elliptical contour for $\boldsymbol{\mu}$ such that

$$(\mathbf{z}-\boldsymbol{\mu})' \left(\frac{\mathbf{\Sigma}}{n}\right)^{-1} (\mathbf{z}-\boldsymbol{\mu}) \leq c^2 \ , \tag{7}$$

delimits a region that will contain $\boldsymbol{\mu}$ with probability α with respect to all possible samples, where $c^2 = \chi^2_2(\alpha)$ is the upper $100\alpha^{\text{th}}$ percentile of the chi-square distribution with two degrees of freedom.

More generally, when the population covariance is unknown, the covariance of the sample-mean can be used instead and the contour equation becomes

$$(\mathbf{z}-\boldsymbol{\mu})'\mathbf{V}_{\mathbf{z}}^{-1}(\mathbf{z}-\boldsymbol{\mu}) \leq c^2 \ , \tag{8}$$

where the constant

$$c^2 = \frac{2(n-1)}{n-2} F_{2,n-2}(\alpha) \tag{9}$$

and $F_{2,n-2}(\alpha)$ is the upper $100\alpha^{\text{th}}$ percentile of the $F_{2,n-2}$ distribution.

2.3.1 Parametric equation for an ellipse

The parametric equation for an ellipse is sometimes useful for plotting elliptical contours. Let a and b be the lengths of the ellipse semi-axes and α the angle of the major semi-axis to the positive x-axis. Then, if (x_0, y_0) is the centre of the ellipse, the following equations describe the contour:

$$\begin{aligned} x &= x_0 + a\cos\alpha\cos t - b\sin\alpha\sin t \\ y &= y_0 + a\sin\alpha\cos t + b\cos\alpha\sin t \end{aligned} \tag{10}$$

where t ranges over angles from zero to 2π.

2.4 An example: impedance

The *Guide* [1], in Appendix H.2, provides an example of the measurement of impedance in an ac circuit. The *Guide*'s treatment of the data does not make use of bivariate statistics so it is interesting to apply them here.

The raw data consist of $n = 5$ simultaneous measurements of voltage, current and the phase of voltage with respect to current (all scalar quantities). The following table reports these values as well as the two components of the bivariate (phasor) impedance, assuming the current is a zero-phase reference. These two components are

$$z_1 = (v/i)\cos\phi$$

and

$$z_2 = (v/i)\sin\phi \ .$$

k	v (volts)	i (milliamps)	ϕ (radians)	z_1 (ohms)	z_2 (ohms)
1	5.007	19.663	1.0456	127.67	220.32
2	4.994	19.639	1.0438	127.89	219.79
3	5.005	19.640	1.0468	127.51	220.64
4	4.990	19.685	1.0428	127.71	218.97
5	4.999	19.678	1.0433	127.88	219.51

From this data the mean impedance is

$$\mathbf{z} = [127.73 \quad 219.85]' \quad (\text{ohms})$$

and the covariance matrix for the mean is

$$\mathbf{V_z} = \begin{bmatrix} 0.508 \times 10^{-2} & -1.239 \times 10^{-2} \\ -1.239 \times 10^{-2} & 8.731 \times 10^{-2} \end{bmatrix},$$

in which each element has the units of (ohms^2).

The eigenvalue-eigenvector pairs for this covariance matrix are

$$\left(3.25 \times 10^{-3}, \begin{bmatrix} \text{-0.989} \\ \text{-0.146} \end{bmatrix}\right), \left(8.91 \times 10^{-2}, \begin{bmatrix} \text{-0.146} \\ \text{0.989} \end{bmatrix}\right)$$

Figure 1 shows the contour of a 95% confidence region superimposed on the raw data ('+') and the mean value ('$\times$'). The contour is calculated using the value for $F_{2,3}(95) = 19.16$, so $c^2 = 51.09$, and the semi-axis lengths are 0.204 and 1.067. The angle between the major axis and the x-axis is 1.72 radians (98 degrees)[1].

Figure 1: A 95% confidence region for the mean of the complex-valued impedance.

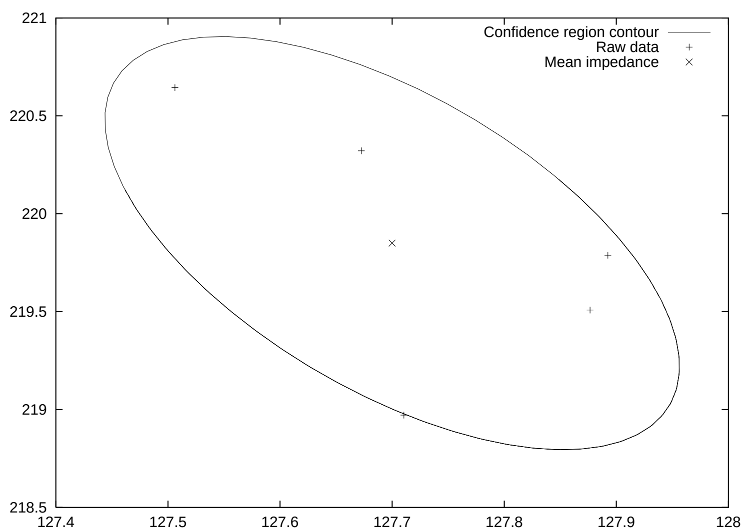

These results are compatible with those from the *Guide* (Table H.3). The components of **z** are equal to the *Guide*'s estimates of resistance and reactance and the associated variances agree.

[1] The components $\cos\alpha$ and $\sin\alpha$ are in fact the components of the eigenvector $[-0.146, \ 0.989]'$ for the larger eigenvalue.

3 Propagation of uncertainty

This section looks at the propagation of uncertainty for two-component data.

3.1 Propagating bivariate uncertainties

The Gaussian law for propagation of variance has a convenient and compact matrix notation, which has been concisely presented by Weise [2]. For this section of the report the following simplified assumptions and notation have been adopted:

- A bivariate function defines the relationship between the inputs and output of a measurement model[2]

$$\mathbf{y} = \mathbf{g}(\mathbf{x}_1, \cdots, \mathbf{x}_n) \ . \tag{11}$$

- The n input quantities $\mathbf{x}_j$, are two-component column vectors $[x_{1j},\ x_{2j}]'$. So it is possible to think of the arguments to $\mathbf{g}$ as forming a single $2n$-component vector

$$\mathbf{x} = [\mathbf{x}_1{}', \mathbf{x}_2{}', \cdots, \mathbf{x}_n{}']' = [x_{11}, x_{21}, x_{12}, \cdots, x_{1n}, x_{2n}]' \ ,$$

  where the element x_{ij} is the i^{th} component (real or imaginary) of the j^{th} input.

- The output quantity $\mathbf{y}$ is a two-component vector $[y_1,\ y_2]'$.
- $\mathbf{g}$ is approximately linear, on the scale of the variability of the input quantities, so it can be expanded in a two-dimensional Taylor series, truncated at linear terms. The partial derivatives are evaluated at the values of $\mathbf{x}_1, \cdots, \mathbf{x}_n$.
- There is a ($2n \times 2n$) input variance-covariance matrix $\mathbf{V_x}$. (Note the variance-covariance matrix elements refer to estimates of the mean.)
- There is a (2×2) variance-covariance matrix $\mathbf{V_y}$ associated with the output.

The output covariance matrix is obtained by evaluating the matrix product [2]

$$\mathbf{V_y} = \frac{\partial \mathbf{g}}{\partial \mathbf{x}'}\, \mathbf{V_x} \left(\frac{\partial \mathbf{g}}{\partial \mathbf{x}'} \right)' \ , \tag{12}$$

where $\frac{\partial \mathbf{g}}{\partial \mathbf{x}'}$ is the $2 \times 2n$ Jacobian matrix of the function $\mathbf{g}$ with respect to $\mathbf{x}$,

$$\frac{\partial \mathbf{g}}{\partial \mathbf{x}'} \equiv \begin{bmatrix} \frac{\partial g_1}{\partial x_{11}} & \frac{\partial g_1}{\partial x_{21}} & \frac{\partial g_1}{\partial x_{12}} & \frac{\partial g_1}{\partial x_{22}} & \cdots & \frac{\partial g_1}{\partial x_{1n}} & \frac{\partial g_1}{\partial x_{2n}} \\ \frac{\partial g_2}{\partial x_{11}} & \frac{\partial g_2}{\partial x_{21}} & \frac{\partial g_2}{\partial x_{12}} & \frac{\partial g_2}{\partial x_{22}} & \cdots & \frac{\partial g_2}{\partial x_{1n}} & \frac{\partial g_2}{\partial x_{2n}} \end{bmatrix} \ . \tag{13}$$

3.2 The standard deviation matrix

The covariance matrix of the inputs can be re-factored into a diagonal 'standard deviation' matrix and a matrix of correlation coefficients. For the $2n \times 2n$ symmetric

[2] The bivariate function $\mathbf{g}$ comprises a pair of scalar functions: $y_1 = g_1(\cdots)$ and $y_2 = g_2(\cdots)$, one for each component.

covariance matrix

$$\mathbf{V_x} = \begin{bmatrix} v_{11\,11} & v_{11\,21} & \cdots & v_{11\,1n} & v_{11\,2n} \\ v_{21\,11} & v_{21\,21} & \cdots & v_{21\,1n} & v_{21\,2n} \\ \vdots & \vdots & \ddots & \vdots & \vdots \\ v_{1n\,11} & v_{1n\,21} & \cdots & v_{1n\,1n} & v_{1n\,2n} \\ v_{2n\,11} & v_{2n\,21} & \cdots & v_{2n\,1n} & v_{2n\,2n} \end{bmatrix}, \tag{14}$$

the standard deviation matrix is the $2n \times 2n$ diagonal matrix

$$\mathbf{S_x} = \begin{bmatrix} \sqrt{v_{11\,11}} & 0 & \cdots & 0 & 0 \\ 0 & \sqrt{v_{21\,21}} & \cdots & 0 & 0 \\ \vdots & \vdots & \ddots & \vdots & \vdots \\ 0 & 0 & \cdots & \sqrt{v_{1n\,1n}} & 0 \\ 0 & 0 & \cdots & 0 & \sqrt{v_{2n\,2n}} \end{bmatrix}, \tag{15}$$

and the matrix of correlation coefficients is

$$\mathbf{R_x} = \begin{bmatrix} 1 & r_{11\,21} & \cdots & r_{11\,1n} & r_{11\,2n} \\ r_{21\,11} & 1 & \cdots & r_{21\,1n} & r_{21\,2n} \\ \vdots & \vdots & \ddots & \vdots & \vdots \\ r_{1n\,11} & r_{1n\,21} & \cdots & 1 & r_{1n\,2n} \\ r_{2n\,11} & r_{2n\,21} & \cdots & r_{2n\,1n} & 1 \end{bmatrix}, \tag{16}$$

where $r_{ij\,kl} = v_{ij\,kl} / \sqrt{v_{ij\,ij} v_{kl\,kl}}$.

Equation (12) can be re-written terms of these matrices

$$\mathbf{V_y} = \frac{\partial \mathbf{g}}{\partial \mathbf{x}'} \, \mathbf{S_x} \, \mathbf{R_x} \, \mathbf{S_x} \left(\frac{\partial \mathbf{g}}{\partial \mathbf{x}'} \right)' . \tag{17}$$

Moreover, the product $\frac{\partial \mathbf{g}}{\partial \mathbf{x}'} \mathbf{S_x}$ can be conveniently referred to as

$$\mathbf{U_x} = \begin{bmatrix} u_{1\cdot 11} & u_{1\cdot 21} & u_{1\cdot 12} & u_{1\cdot 22} & \cdots & u_{1\cdot 1n} & u_{1\cdot 2n} \\ u_{2\cdot 11} & u_{2\cdot 21} & u_{2\cdot 12} & u_{2\cdot 22} & \cdots & u_{2\cdot 1n} & u_{2\cdot 2n} \end{bmatrix}, \tag{18}$$

where each column of $\frac{\partial \mathbf{g}}{\partial \mathbf{x}'}$ has been multiplied by $\sqrt{v_{kl\,kl}}$, i.e.

$$u_{i\cdot kl} = \sqrt{v_{kl\,kl}} \, \frac{\partial g_i}{\partial x_{kl}} .$$

This allows equation (17) to be expressed in the alternative form

$$\mathbf{V_y} = \mathbf{U_x} \, \mathbf{R_x} \, \mathbf{U_x'} . \tag{19}$$

3.2.1 An example: impedance (continued)

The raw data from the table in Section 2.4 can be used to obtain the mean values of voltage (v), current (i) and phase (ϕ), together with their standard deviations and correlation coefficients. Let $x_{11} = v$, $x_{12} = i$ and $x_{13} = \phi$. The associated imaginary components (x_{21}, x_{22}, x_{23}) are all zero. The calculated values are (the notation $u(x_i)$ indicates the standard uncertainty in x_i):

$$x_{11} = 4.9990 \quad u(x_{11}) = 3.209\text{E-3} \quad \text{(volts)}$$
$$x_{12} = 19.6610\text{E-3} \quad u(x_{12}) = 9.471\text{E-6} \quad \text{(amps)}$$
$$x_{13} = 1.04446 \quad u(x_{13}) = 7.521\text{E-4} \quad \text{(radians)}$$

$$r_{11\,12} = -0.36$$
$$r_{11\,13} = 0.86$$
$$r_{12\,13} = -0.65$$

The bivariate function for $\mathbf{z}$ is then

$$\mathbf{z} = \mathbf{g}(\mathbf{x}_1, \mathbf{x}_2, \mathbf{x}_3) = \begin{bmatrix} \frac{x_{11}}{x_{12}} \cos x_{13} \\ \frac{x_{11}}{x_{12}} \sin x_{13} \end{bmatrix} .$$

The (2×6) Jacobian matrix for $\mathbf{g}$ is [3]

$$\frac{\partial \mathbf{g}}{\partial \mathbf{x}'} = \begin{bmatrix} \frac{\cos x_{13}}{x_{12}} & 0 & -\frac{x_{11}}{x_{12}^2} \cos x_{13} & 0 & -\frac{x_{11}}{x_{12}} \sin x_{13} & 0 \\ \frac{\sin x_{13}}{x_{12}} & 0 & -\frac{x_{11}}{x_{12}^2} \sin x_{13} & 0 & \frac{x_{11}}{x_{12}} \cos x_{13} & 0 \end{bmatrix} ,$$

and substituting for the values in this case yields

$$\frac{\partial \mathbf{g}}{\partial \mathbf{x}'} = \begin{bmatrix} 25.55 & 0 & -6498 & 0 & -219.8 & 0 \\ 43.98 & 0 & -11,182 & 0 & 127.7 & 0 \end{bmatrix} .$$

Multiplying by the standard deviation matrix one obtains

$$\mathbf{U}_{\mathbf{x}} = \begin{bmatrix} 0.08200 & 0 & -0.0615 & 0 & -0.1653 & 0 \\ 0.1411 & 0 & -0.1059 & 0 & 0.0960 & 0 \end{bmatrix} .$$

Using the (6×6) correlation matrix

$$\mathbf{R}_{\mathbf{x}} = \begin{bmatrix} 1 & 0 & -0.36 & 0 & 0.86 & 0 \\ 0 & 1 & 0 & 0 & 0 & 0 \\ -0.36 & 0 & 1 & 0 & -0.65 & 0 \\ 0 & 0 & 0 & 1 & 0 & 0 \\ 0.86 & 0 & -0.65 & 0 & 1 & 0 \\ 0 & 0 & 0 & 0 & 0 & 1 \end{bmatrix} ,$$

one obtains the covariance for $\mathbf{z}$ as

$$\mathbf{V}_{\mathbf{z}} = \begin{bmatrix} 0.493 \times 10^{-2} & -1.237 \times 10^{-2} \\ -1.237 \times 10^{-2} & 8.767 \times 10^{-2} \end{bmatrix} .$$

These values are in close agreement with the covariance matrix elements found in Section 2.4.

Note, however, that we have used two alternative ways of processing the data which are not equivalent. The *Guide* takes a similar approach. In this section, the data was reduced to a single triplet of voltage current and phase, by taking the means of the measurements in each quantity, and then the impedance was estimated. This is similar to the *Guide*'s first approach to the problem in Appendix H. In Section 2.4, the complex components of impedance were found for each triplet of data and then the mean value was calculated. That is analogous to the second approach used in the *Guide*.

[3] The three matrix columns associated with the second components of the inputs are clearly redundant here. They are included to explicitly match the general form of the matrix notation being employed.

3.3 Complex derivatives and the Jacobian matrix

Complex numbers are frequently used in engineering and physical science to represent bivariate data. They provide a convenient framework for many kinds of calculations. The basic arithmetic operations are defined on the set of complex numbers, as are many standard mathematical functions (e.g., $\sin$, $\exp$, etc). Furthermore, the rules that apply to differentiation of complex numbers are nearly the same as those for real numbers [10]. This section looks at the correspondence between complex derivatives and the equivalent bivariate Jacobian matrix representation.

Although complex numbers have two components, it is useful to make a distinction between a complex number and the 2-component vector representation of bivariate data used so far.[4] Bold italic characters are used to represent a complex number or a function returning a complex number, e.g.: $\boldsymbol{z} = x_1 + j\, x_2$ (for x_1, x_2 real).

A function $\boldsymbol{g}(\boldsymbol{z})$ of a complex variable $\boldsymbol{z}$ can be defined quite generally using two scalar functions

$$\boldsymbol{g}(\boldsymbol{z}) = g_1(x_1, x_2) + j\, g_2(x_1, x_2) \ . \tag{20}$$

The corresponding Jacobian matrix is

$$\frac{\partial \mathbf{y}}{\partial \mathbf{x}'} = \begin{bmatrix} \frac{\partial g_1}{\partial x_1} & \frac{\partial g_1}{\partial x_2} \\ \frac{\partial g_2}{\partial x_1} & \frac{\partial g_2}{\partial x_2} \end{bmatrix}$$

This matrix of four elements is really reducd to two by the Cauchy-Riemann relations [10]

$$\frac{\partial g_1}{\partial x_1} = \frac{\partial g_2}{\partial x_2} \quad , \quad \frac{\partial g_1}{\partial x_2} = -\frac{\partial g_2}{\partial x_1} \ . \tag{21}$$

The diagonal terms of the Jacobian matrix are equal and the off-diagonal terms are of equal magnitude but opposite sign.

This suggests a simple mapping from a complex number to a matrix. For any complex number $\boldsymbol{z} = a + j\, b$ (for a, b real)

$$\mathbf{M}(\mathbf{z}) \equiv \begin{bmatrix} a & -b \\ b & a \end{bmatrix} \ . \tag{22}$$

The matrix representation generated by this mapping reproduces the complex arithmetic operations by the rules of linear algebra. Note also that the matrix transpose is equivalent to the complex conjugate

$$\mathbf{M}(\mathbf{z})' \equiv \mathbf{M}(\mathbf{z}^*) \ .$$

The Jacobian matrix in equation (13) can now be generated from the individual complex derivatives by applying this mapping

$$\frac{\partial \boldsymbol{g}}{\partial \boldsymbol{x}'} = \begin{bmatrix} \mathbf{M}\left(\frac{\partial \boldsymbol{g}}{\partial \boldsymbol{x}_1}\right) & \mathbf{M}\left(\frac{\partial \boldsymbol{g}}{\partial \boldsymbol{x}_2}\right) & \cdots & \mathbf{M}\left(\frac{\partial \boldsymbol{g}}{\partial \boldsymbol{x}_n}\right) \end{bmatrix} \ . \tag{23}$$

[4] The need to distinguish between complex numbers and 2-component vectors becomes clear when one remembers that the product of two bivariate vectors is undefined!

3.3.1 An example: multiplication

To illustrate the relation between the linear algebra, complex numbers and the Jacobian matrix, consider the operation of multiplication.

Let $\boldsymbol{y} = \boldsymbol{x}_1 \, \boldsymbol{x}_2$, where $\boldsymbol{x}_1 = x_{11} + j\, x_{21}$ and $\boldsymbol{x}_2 = x_{12} + j\, x_{22}$. If we consider $\boldsymbol{x} \equiv [\boldsymbol{x}_1, \boldsymbol{x}_2]'$ then the *complex* Jacobian matrix is

$$\frac{\partial \boldsymbol{y}}{\partial \boldsymbol{x}'} = \left[\begin{array}{cc} \boldsymbol{x}_2 & \boldsymbol{x}_1 \end{array} \right] .$$

The linear algebra approach considers the two components of $\boldsymbol{y}$ to be functions of the 4-vector $[x_{11}, x_{21}, x_{12}, x_{22}]'$, i.e.

$$y_1 = x_{11}\, x_{12} - x_{21}\, x_{22}$$

$$y_2 = x_{11}\, x_{22} + x_{12}\, x_{21}$$

The Jacobian matrix is therefore the 2×4 matrix

$$\frac{\partial \mathbf{y}}{\partial \mathbf{x}'} = \left[\begin{array}{cccc} x_{12} & -x_{22} & x_{11} & -x_{21} \\ x_{22} & x_{12} & x_{21} & x_{11} \end{array} \right] .$$

4 Vector Network Analyzer calibration

This section reviews some of the network analysis that applies to VNA calibration. There are many procedures for calibrating VNAs, essentially differing in the number and type of standard artifacts. There are also two distinct hardware configurations for VNAs: 4-sampler and 3-sampler.

A 4-sampler VNA has four receiver channels, allowing simultaneous measurement of the incident signal at the first port, the reflected signal from the first port, the incident signal at the second port and the reflected signal from the second port.

A 3-sampler VNA cannot measure the reflected signal from the second port (that is, the port opposite the one at which signal is applied). Nevertheless a 3-sampler VNA changes configuration internally to perform 'forward' and 'reverse' measurements. As a consequence, the calibration procedure must consider both configurations separately [3].

Woods was the first to *formally* derive the equations pertinent to 3-sampler VNA calibration [4]. His analysis used scattering matrices to describe the directional couplers and other linear elements of a VNA. However, it is common for calibration procedures to refer instead to n-term 'error models', represented by signal flow-graphs. In the case of the 3-sampler VNA, the '12-term error model' is conventional.

This section breaks temporarily with the notation used earlier, in order to adopt the conventional engineering presentation of the topic. All quantities in this section should be considered complex-valued. Subscripts identify matrix, or vector, elements but bold typeface is not used to represent entire matrices or vectors. There is no strict rule regarding the use of upper or lowercase symbols either!

4.1 The 3-term error model

The 3-term error model for a single reflectometer port is shown in Fig. 2. The error terms are:

- E_D: the 'directivity', comprising leakage and reflections inherent in the couplers, test cables, etc;
- E_S: the source 'match', comprising adaptor and cable effects;
- E_R: the 'reflection tracking', comprising coupler sampler and test cable response.

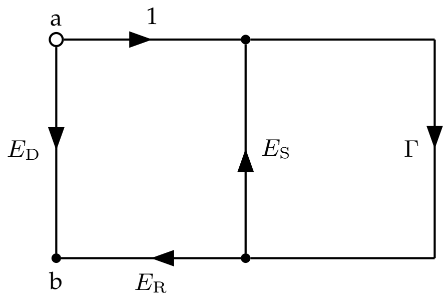

Figure 2: The 1-port error model has three complex error correction coefficients. The external reflection coefficient Γ is seen by the port during measurement.

4.1.1 3-term error model correction equations

Once the error terms have been obtained, VNA readings can be corrected. The correction equation is:

$$\Gamma = \frac{\Gamma^\mathrm{m} - E_\mathrm{D}}{E_\mathrm{S}(\Gamma^\mathrm{m} - E_\mathrm{D}) + E_\mathrm{R}} \; . \tag{24}$$

4.2 The 12-term error model

The 12-term error model for a 3-sampler VNA is shown in Fig. 3. The figure has two diagrams, one for each configuration of the VNA.

The terms are (a second subscript F or R indicates 'forward' or 'reverse' configuration) [3]

- E_D: the 'directivity', comprising leakage and reflections inherent in the couplers, test cables, etc;
- E_S: the source 'match', comprising adaptor and cable effects;
- E_R: the 'reflection tracking', comprising coupler sampler and test cable responses;
- E_X: the transmission leakage, arising from crosstalk in mixers and switches;
- E_T: the transmission 'tracking';
- E_L: the load match.

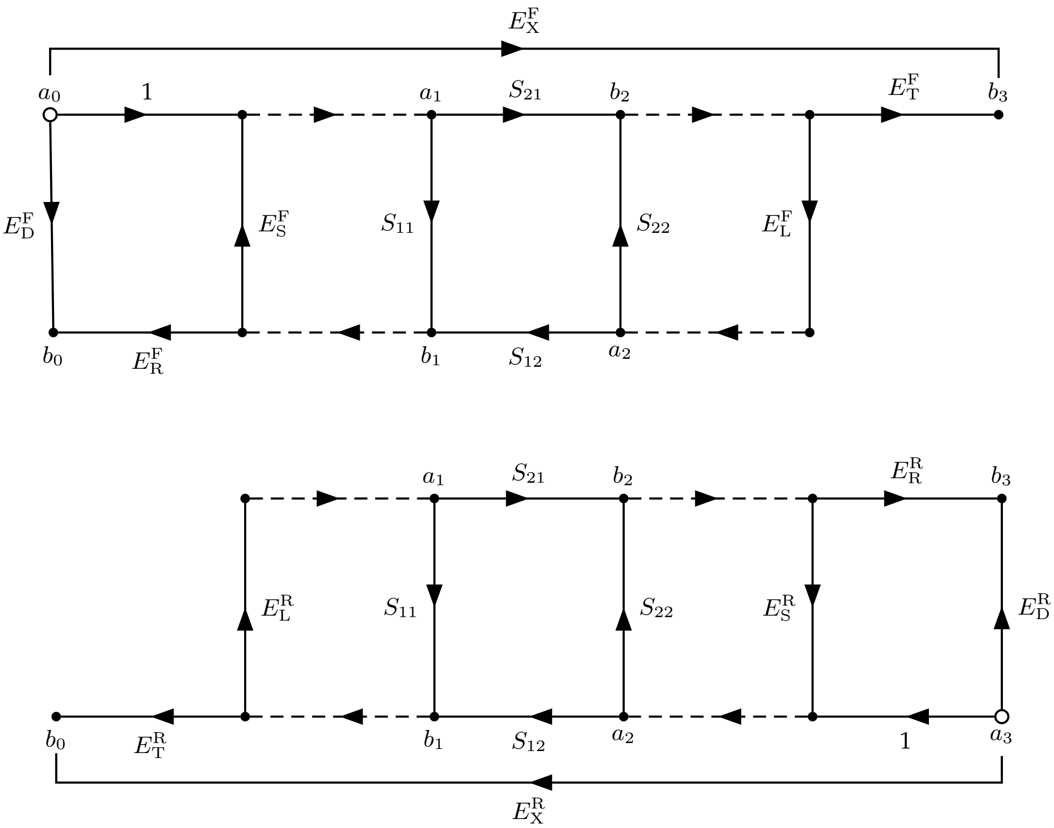

Figure 3: Signal flow diagrams for the '12-term' error model. The upper diagram applies to the 'forward' VNA configuration, while the lower diagram applies to the 'reverse'. Signal is introduced at the open-circle node in each diagram. The S_{ij} are S-parameters of a calibration artifact connected between the measurement ports.

4.2.1 12-term error model correction equations

Once the error terms have been obtained, VNA readings can be corrected. The four correction equations are [5, 8](a derivation is also given in [3])

$$
\begin{aligned}
S_{11} &= \frac{b_0}{a_0} \\
&= \frac{\left\{\left(\frac{S_{11}^{\mathrm{M}}-E_{\mathrm{D}}^{\mathrm{F}}}{E_{\mathrm{R}}^{\mathrm{F}}}\right)\left[1+\left(\frac{S_{22}^{\mathrm{M}}-E_{\mathrm{D}}^{\mathrm{R}}}{E_{\mathrm{R}}^{\mathrm{R}}}\right)E_{\mathrm{S}}^{\mathrm{R}}\right]\right\}-\left[\left(\frac{S_{21}^{\mathrm{M}}-E_{\mathrm{X}}^{\mathrm{F}}}{E_{\mathrm{T}}^{\mathrm{F}}}\right)\left(\frac{S_{12}^{\mathrm{M}}-E_{\mathrm{X}}^{\mathrm{R}}}{E_{\mathrm{T}}^{\mathrm{R}}}\right)E_{\mathrm{L}}^{\mathrm{F}}\right]}{\left[1+\left(\frac{S_{11}^{\mathrm{M}}-E_{\mathrm{D}}^{\mathrm{F}}}{E_{\mathrm{R}}^{\mathrm{F}}}\right)E_{\mathrm{S}}^{\mathrm{F}}\right]\left[1+\left(\frac{S_{22}^{\mathrm{M}}-E_{\mathrm{D}}^{\mathrm{R}}}{E_{\mathrm{R}}^{\mathrm{R}}}\right)E_{\mathrm{S}}^{\mathrm{R}}\right]-\left[\left(\frac{S_{21}^{\mathrm{M}}-E_{\mathrm{X}}^{\mathrm{F}}}{E_{\mathrm{T}}^{\mathrm{F}}}\right)\left(\frac{S_{12}^{\mathrm{M}}-E_{\mathrm{X}}^{\mathrm{R}}}{E_{\mathrm{T}}^{\mathrm{R}}}\right)E_{\mathrm{L}}^{\mathrm{F}}E_{\mathrm{L}}^{\mathrm{R}}\right]}
\end{aligned} \tag{25}
$$

$$
\begin{aligned}
S_{21} &= \frac{b_3}{a_0} \\
&= \frac{\left[1+\left(\frac{S_{22}^{\mathrm{M}}-E_{\mathrm{D}}^{\mathrm{R}}}{E_{\mathrm{R}}^{\mathrm{R}}}\right)\left(E_{\mathrm{S}}^{\mathrm{R}}-E_{\mathrm{L}}^{\mathrm{F}}\right)\right]\left(\frac{S_{21}^{\mathrm{M}}-E_{\mathrm{X}}^{\mathrm{F}}}{E_{\mathrm{T}}^{\mathrm{F}}}\right)}{\left[1+\left(\frac{S_{11}^{\mathrm{M}}-E_{\mathrm{D}}^{\mathrm{F}}}{E_{\mathrm{R}}^{\mathrm{F}}}\right)E_{\mathrm{S}}^{\mathrm{F}}\right]\left[1+\left(\frac{S_{22}^{\mathrm{M}}-E_{\mathrm{D}}^{\mathrm{R}}}{E_{\mathrm{R}}^{\mathrm{R}}}\right)E_{\mathrm{S}}^{\mathrm{R}}\right]-\left[\left(\frac{S_{21}^{\mathrm{M}}-E_{\mathrm{X}}^{\mathrm{F}}}{E_{\mathrm{T}}^{\mathrm{F}}}\right)\left(\frac{S_{12}^{\mathrm{M}}-E_{\mathrm{X}}^{\mathrm{R}}}{E_{\mathrm{T}}^{\mathrm{R}}}\right)E_{\mathrm{L}}^{\mathrm{F}}E_{\mathrm{L}}^{\mathrm{R}}\right]}
\end{aligned} \tag{26}
$$

$$S_{12} = \frac{b_0}{a_3} \tag{27}$$

$$= \frac{\left[1+\left(\frac{S_{11}^{\rm M}-E_{\rm D}^{\rm F}}{E_{\rm R}^{\rm F}}\right)\left(E_{\rm S}^{\rm F}-E_{\rm L}^{\rm R}\right)\right]\left(\frac{S_{12}^{\rm M}-E_{\rm X}^{\rm R}}{E_{\rm T}^{\rm R}}\right)}{\left[1+\left(\frac{S_{11}^{\rm M}-E_{\rm D}^{\rm F}}{E_{\rm R}^{\rm F}}\right)E_{\rm S}^{\rm F}\right]\left[1+\left(\frac{S_{22}^{\rm M}-E_{\rm D}^{\rm R}}{E_{\rm R}^{\rm R}}\right)E_{\rm S}^{\rm R}\right]-\left[\left(\frac{S_{21}^{\rm M}-E_{\rm X}^{\rm F}}{E_{\rm T}^{\rm F}}\right)\left(\frac{S_{12}^{\rm M}-E_{\rm X}^{\rm R}}{E_{\rm T}^{\rm R}}\right)E_{\rm L}^{\rm F}E_{\rm L}^{\rm R}\right]}$$

$$S_{22} = \frac{b_3}{a_3} \tag{28}$$

$$= \frac{\left\{\left(\frac{S_{22}^{\rm M}-E_{\rm D}^{\rm R}}{E_{\rm R}^{\rm R}}\right)\left[1+\left(\frac{S_{11}^{\rm M}-E_{\rm D}^{\rm F}}{E_{\rm R}^{\rm F}}\right)E_{\rm S}^{\rm F}\right]\right\}-\left[\left(\frac{S_{21}^{\rm M}-E_{\rm X}^{\rm F}}{E_{\rm T}^{\rm F}}\right)\left(\frac{S_{12}^{\rm M}-E_{\rm X}^{\rm R}}{E_{\rm T}^{\rm R}}\right)E_{\rm L}^{\rm R}\right]}{\left[1+\left(\frac{S_{11}^{\rm M}-E_{\rm D}^{\rm F}}{E_{\rm R}^{\rm F}}\right)E_{\rm S}^{\rm F}\right]\left[1+\left(\frac{S_{22}^{\rm M}-E_{\rm D}^{\rm R}}{E_{\rm R}^{\rm R}}\right)E_{\rm S}^{\rm R}\right]-\left[\left(\frac{S_{21}^{\rm M}-E_{\rm X}^{\rm F}}{E_{\rm T}^{\rm F}}\right)\left(\frac{S_{12}^{\rm M}-E_{\rm X}^{\rm R}}{E_{\rm T}^{\rm R}}\right)E_{\rm L}^{\rm F}E_{\rm L}^{\rm R}\right]}$$

4.3 Network analysis for OSLT calibration

In calibration, the twelve error terms are determined by a series of raw VNA measurements of previously characterized physical artifacts. This can be accomplished in a two-step process, called 'Open-Short-Load-Thru' (OSLT) calibration procedure.[5] First, 1-port artifacts are connected to each VNA measurement port, thereby isolating the forward and reverse $E_{\rm D}$, $E_{\rm R}$ and $E_{\rm S}$ terms. Second, a 2-port artifact is used to determine $E_{\rm L}$ and $E_{\rm T}$.

4.3.1 1-port error terms

In either the forward or reverse VNA configuration, connecting a 1-port device to the test port simplifies the error model, as shown in Fig. 2

A VNA reflection coefficient measurement determines the ratio of the complex values of a and b[6], so

$$\begin{aligned}\Gamma^{\rm m} &= \frac{b}{a} \\ &= E_{\rm D} + \frac{E_{\rm R}\,\Gamma}{1-E_{\rm S}\,\Gamma} \\ &= \frac{E_{\rm D}+(E_{\rm R}-E_{\rm D}E_{\rm S})\Gamma}{1-E_{\rm S}\,\Gamma} \\ &= \frac{A\Gamma+B}{C\,\Gamma+1}\;.\end{aligned} \tag{29}$$

Three reflection artifacts, Γ_1, Γ_2 and Γ_3, are required to determine the error terms. Equation (29) is linear in the three complex constants A, B and C, and can be re-written as

$$A\,\Gamma_i + B - \Gamma_i^{\rm m}\,\Gamma_i\,C = \Gamma_i^{\rm m}\;, \tag{30}$$

[5] Recently, several other calibration schemes were proposed for 3-sampler VNAs [6]. These procedures are not discussed in this report, however they may merit further attention. In particular, they may offer the advantage of requiring standard artifacts that can be more readily characterised and more stable. If so, it may be feasible to send a set of artifacts for characterization and later use them to calibrate the VNA remotely. This general approach to VNA calibration is already offered for 4-sampler VNAs by NPL.

[6] In the forward configuration, the measured reflection coefficient is the S_{11} parameter; in the reverse, it is S_{22}.

or in matrix form

$$\begin{bmatrix} \Gamma_1 & 1 & -\Gamma^{\mathrm{m}}_1 \Gamma_1 \\ \Gamma_2 & 1 & -\Gamma^{\mathrm{m}}_2 \Gamma_2 \\ \Gamma_3 & 1 & -\Gamma^{\mathrm{m}}_3 \Gamma_3 \end{bmatrix} \begin{bmatrix} A \\ B \\ C \end{bmatrix} = \begin{bmatrix} \Gamma^{\mathrm{m}}_1 \\ \Gamma^{\mathrm{m}}_2 \\ \Gamma^{\mathrm{m}}_3 \end{bmatrix} . \tag{31}$$

To refer to the components of complex quantities we use a notation in which the real component has a leading subscript '1' and the imaginary component '2'. So, for example, the real and imaginary components of A are A_1 and A_2, respectively, and the components of the i^{th} measured reflection coefficient are Γ^{m}_{1i} and Γ^{m}_{2i}.

In this notation, (30) can be written as a pair of scalar equations:

$$\begin{aligned} \Gamma_{1i} A_1 - \Gamma_{2i} A_2 + B_1 + (\Gamma_{2i} \Gamma^{\mathrm{m}}_{2i} - \Gamma_{1i} \Gamma^{\mathrm{m}}_{1i}) C_1 + (\Gamma_{1i} \Gamma^{\mathrm{m}}_{2i} + \Gamma_{2i} \Gamma^{\mathrm{m}}_{1i}) C_2 &= \Gamma^{\mathrm{m}}_{1i} , \\ \Gamma_{2i} A_1 + \Gamma_{1i} A_2 + B_2 - (\Gamma_{1i} \Gamma^{\mathrm{m}}_{2i} + \Gamma_{2i} \Gamma^{\mathrm{m}}_{1i}) C_1 + (\Gamma_{2i} \Gamma^{\mathrm{m}}_{2i} - \Gamma_{1i} \Gamma^{\mathrm{m}}_{1i}) C_2 &= \Gamma^{\mathrm{m}}_{2i} . \end{aligned}$$

Equation (31) can be solved by standard techniques of linear algebra. Having obtained values for A, B and C the error terms are simply

$$\begin{aligned} E_{\mathrm{D}} &= B , \\ E_{\mathrm{S}} &= -C , \\ E_{\mathrm{R}} &= A - BC . \end{aligned}$$

4.3.2 2-port error terms

To facilitate the analysis when a 2-port device is connected between the measurement ports, the 1-port error terms can be combined with the S-parameters of an arbitrary 2-port artifact [5]. This simplifies the signal flow graph, as shown in Fig. 4.

The error terms $E^{\mathrm{F}}_{\mathrm{L}}$, $E^{\mathrm{R}}_{\mathrm{L}}$, $E^{\mathrm{F}}_{\mathrm{T}}$ and $E^{\mathrm{F}}_{\mathrm{T}}$ can be obtained by measuring the four S-parameters (raw measurements are denoted S^{m}_{ij}) of a well-characterized 2-port artifact

$$E^{\mathrm{F}}_{\mathrm{L}} = \frac{S^{\mathrm{m}}_{11} - S^{\mathrm{F}}_{11}}{S^{\mathrm{F}}_{22}(S^{\mathrm{m}}_{11} - S^{\mathrm{F}}_{11}) + S^{\mathrm{F}}_{21} S^{\mathrm{F}}_{12}} , \tag{32}$$

$$E^{\mathrm{R}}_{\mathrm{L}} = \frac{S^{\mathrm{m}}_{22} - S^{\mathrm{R}}_{22}}{S^{\mathrm{R}}_{11}(S^{\mathrm{m}}_{22} - S^{\mathrm{R}}_{22}) + S^{\mathrm{R}}_{21} S^{\mathrm{R}}_{12}} , \tag{33}$$

$$E^{\mathrm{F}}_{\mathrm{T}} = \frac{(S^{\mathrm{m}}_{21} - E^{\mathrm{F}}_{X})(1 - E^{\mathrm{F}}_{L} S^{\mathrm{F}}_{22})}{S^{\mathrm{F}}_{21}} , \tag{34}$$

$$E^{\mathrm{R}}_{\mathrm{T}} = \frac{(S^{\mathrm{m}}_{12} - E^{\mathrm{R}}_{X})(1 - E^{\mathrm{R}}_{L} S^{\mathrm{R}}_{11})}{S^{\mathrm{R}}_{12}} . \tag{35}$$

The leakage terms, $E^{\mathrm{F}}_{\mathrm{X}}$ and $E^{\mathrm{R}}_{\mathrm{X}}$, can be determined by connecting a load to each VNA port and measuring the transmission coefficients

$$E^{\mathrm{F}}_{\mathrm{X}} = \frac{b_3}{a_0} = S^{\mathrm{m}}_{21} , \tag{36}$$

$$E^{\mathrm{R}}_{\mathrm{X}} = \frac{b_0}{a_3} = S^{\mathrm{m}}_{12} . \tag{37}$$

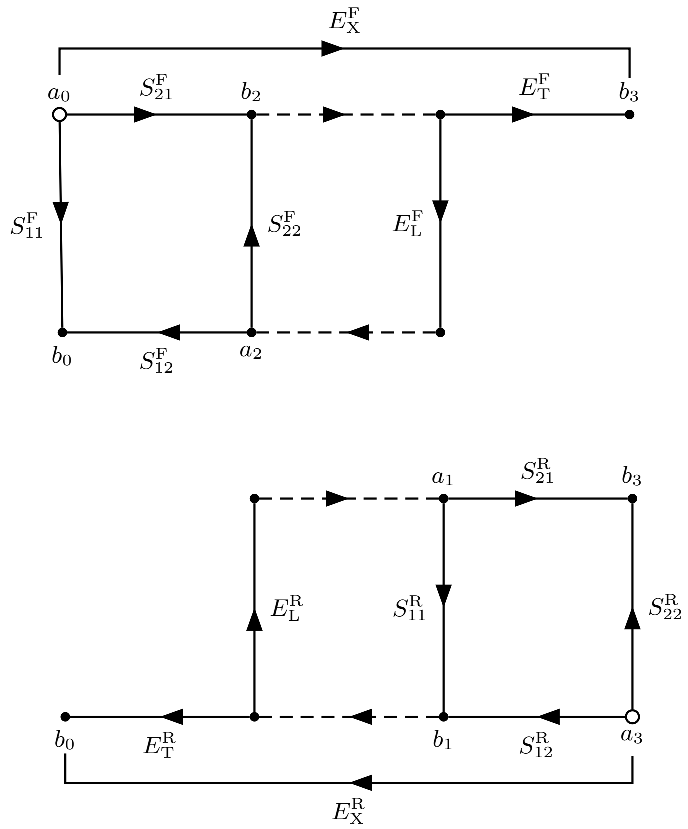

Figure 4: The flow diagram of Fig. 3 can be simplified by cascading the 1-port error terms with S-parameters of the 2-port artifact.

4.3.3 Cascaded terms

Equations (32) to (35) use composite 2-port S-parameters representing the combination of error terms and the artifact S-parameters (S_{ij}). These terms are now given explicitly. They can be classified into two groups, one for each VNA configuration.

For the forward configuration:

$$S_{11}^{\mathrm{F}} = E_{\mathrm{D}}^{\mathrm{F}} + \frac{E_{\mathrm{R}}^{\mathrm{F}}\, S_{11}}{1 - E_{\mathrm{S}}^{\mathrm{F}}\, S_{11}} \equiv \frac{A^{\mathrm{F}} S_{11} + B^{\mathrm{F}}}{1 + C^{\mathrm{F}} S_{11}} \,, \tag{38}$$

$$S_{21}^{\mathrm{F}} = \frac{S_{21}}{1 - E_{\mathrm{S}}^{\mathrm{F}}\, S_{11}} \equiv \frac{S_{21} + B^{\mathrm{F}}}{1 + C^{\mathrm{F}} S_{11}} \,, \tag{39}$$

$$S_{12}^{\mathrm{F}} = \frac{E_{\mathrm{R}}^{\mathrm{F}}\, S_{12}}{1 - E_{\mathrm{S}}^{\mathrm{F}}\, S_{11}} \equiv \frac{(A^{\mathrm{F}} + B^{\mathrm{F}} C^{\mathrm{F}}) S_{12}}{1 + C^{\mathrm{F}} S_{11}} \,, \tag{40}$$

$$S_{22}^{\mathrm{F}} = S_{22} + \frac{E_{\mathrm{S}}^{\mathrm{F}}\, S_{21}\, S_{12}}{1 - E_{\mathrm{S}}^{\mathrm{F}}\, S_{11}} \equiv \frac{S_{22} + C^{\mathrm{F}} (S_{11} S_{22} - S_{12} S_{21})}{1 + C^{\mathrm{F}} S_{11}} \,. \tag{41}$$

For the reverse:

$$S_{11}^{\mathrm{R}} = S_{11} + \frac{E_{\mathrm{S}}^{\mathrm{R}}\, S_{12}\, S_{21}}{1 - E_{\mathrm{S}}^{\mathrm{R}}\, S_{22}} \equiv \frac{S_{11} + C^{\mathrm{R}} (S_{11} S_{22} - S_{12} S_{21})}{1 + C^{\mathrm{R}} S_{22}} \,, \tag{42}$$

$$S^{\mathrm{R}}_{21} = \frac{E^{\mathrm{R}}_{\mathrm{R}}\, S_{21}}{1 - E^{\mathrm{R}}_{\mathrm{S}}\, S_{22}} \equiv \frac{(A^{\mathrm{R}} + B^{\mathrm{R}} C^{\mathrm{R}}) S_{21}}{1 + C^{\mathrm{R}} S_{22}} \,, \tag{43}$$

$$S^{\mathrm{R}}_{12} = \frac{S_{12}}{1 - E^{\mathrm{R}}_{\mathrm{S}}\, S_{22}} \equiv \frac{S_{12}}{1 + C^{\mathrm{R}} S_{22}} \,, \tag{44}$$

$$S^{\mathrm{R}}_{22} = E^{\mathrm{R}}_{\mathrm{D}} + \frac{E^{\mathrm{R}}_{\mathrm{R}}\, S_{22}}{1 - E^{\mathrm{R}}_{\mathrm{S}}\, S_{22}} \equiv \frac{A^{\mathrm{R}} S_{22} + B^{\mathrm{R}}}{1 + C^{\mathrm{R}} S_{22}} \,. \tag{45}$$

These equations can be derived using cascade matrices, which provide a convenient analysis tool for series networks.[7] The cascade matrix for a series connection of several 2-port devices is the product of the individual cascade matrices.

The relationship between a 2-port cascade matrix and an S-matrix is

$$R = \frac{1}{S_{21}} \begin{bmatrix} (S_{12}S_{21} - S_{11}S_{22}) & S_{11} \\ -S_{22} & 1 \end{bmatrix} \tag{46}$$

and the converse is

$$S = \frac{1}{r_{22}} \begin{bmatrix} r_{12} & (r_{11}r_{22} - r_{12}r_{21}) \\ 1 & -r_{21} \end{bmatrix} \,. \tag{47}$$

When two 2-ports are cascaded, with m to the left of n and the scattering parameters m_{ij} and n_{ij}, the S-parameters of the combination are

$$S_{11} = m_{11} + \frac{m_{12}\, m_{21}\, n_{11}}{1 - m_{22}\, n_{11}} \,, \tag{48}$$

$$S_{21} = \frac{m_{21}\, n_{21}}{1 - m_{22}\, n_{11}} \,, \tag{49}$$

$$S_{12} = \frac{n_{12}\, m_{12}}{1 - n_{11}\, m_{22}} \,, \tag{50}$$

$$S_{22} = n_{22} + \frac{m_{22}\, n_{21}\, n_{12}}{1 - m_{22}\, n_{11}} \,. \tag{51}$$

4.4 Calibration consistency

In principle, the two-step treatment above is not optimal: the twelve error terms could be obtained in a single step, using all of the available measurement and artifact data, by solving a non-linear problem. However, this approach does not seem to have been formulated.

Marks has shown that there is a condition on the 12-term model [8]

$$E^{\mathrm{F}}_{\mathrm{T}} E^{\mathrm{R}}_{T} = [E^{\mathrm{R}}_{\mathrm{R}} + E^{\mathrm{R}}_{\mathrm{D}}(E^{\mathrm{F}}_{\mathrm{L}} - E^{\mathrm{R}}_{\mathrm{S}})]\, [E^{\mathrm{F}}_{\mathrm{R}} + E^{\mathrm{F}}_{\mathrm{D}}(E^{\mathrm{R}}_{\mathrm{L}} - E^{\mathrm{F}}_{\mathrm{S}})] \,. \tag{52}$$

A more elaborate data analysis could use (52) as a constraint on the non-linear problem. Nonetheless, (52) will also be useful as a validation check of the two-step procedure.

Another interesting feature of Marks' analysis is that the reflection coefficient of the internal termination (recall that the 3-sampler hardware must switch one receiver

[7] A description of cascade matrices is given in [7, 2.11].

channel between ports) in the forward and reverse configurations can be expressed explicitly. In the forward configuration

$$\Gamma^{\mathrm{F}} = \frac{E_{\mathrm{L}}^{\mathrm{F}} - E_{\mathrm{S}}^{\mathrm{R}}}{E_{\mathrm{R}}^{\mathrm{R}} + E_{\mathrm{D}}^{\mathrm{R}}(E_{\mathrm{L}}^{\mathrm{F}} - E_{\mathrm{S}}^{\mathrm{R}})} \tag{53}$$

and in the reverse

$$\Gamma^{\mathrm{R}} = \frac{E_{\mathrm{L}}^{\mathrm{R}} - E_{\mathrm{S}}^{\mathrm{F}}}{E_{\mathrm{R}}^{\mathrm{F}} + E_{\mathrm{D}}^{\mathrm{F}}(E_{\mathrm{L}}^{\mathrm{R}} - E_{\mathrm{S}}^{\mathrm{F}})} \ . \tag{54}$$

The values of Γ^{F} and Γ^{R} should be very stable over time for a particular instrument, because they depend essentially on an internal electronic VNA switch.

5 Uncertainty associated with a VNA calibration

This section looks at the uncertainty of the VNA error terms obtained by calibration. The notation now reverts to the use of lowercase bold characters for vectors and uppercase bold for matrices. Note, however, that when referring to quantities introduced in the previous section the original notation is retained – this should not be a problem as only the component values are needed.

5.1 1-port uncertainty

In the first part of section 4.3, a 1-port model was used to obtain six of the twelve error parameters. Recall the matrix form of the calibration equations[8]

$$\begin{bmatrix} \boldsymbol{\Gamma}_1 & 1 & -\boldsymbol{\Gamma}_1 \boldsymbol{\Gamma}_1^{\mathrm{m}} \\ \boldsymbol{\Gamma}_2 & 1 & -\boldsymbol{\Gamma}_2 \boldsymbol{\Gamma}_2^{\mathrm{m}} \\ \boldsymbol{\Gamma}_3 & 1 & -\boldsymbol{\Gamma}_3 \boldsymbol{\Gamma}_3^{\mathrm{m}} \end{bmatrix} \begin{bmatrix} \boldsymbol{A} \\ \boldsymbol{B} \\ \boldsymbol{C} \end{bmatrix} = \begin{bmatrix} \boldsymbol{\Gamma}_1^{\mathrm{m}} \\ \boldsymbol{\Gamma}_2^{\mathrm{m}} \\ \boldsymbol{\Gamma}_3^{\mathrm{m}} \end{bmatrix} \tag{55}$$

or in full scalar notation:

$$\begin{bmatrix} \Gamma_{11} & -\Gamma_{21} & 1 & 0 & (\Gamma_{21}\Gamma_{21}^{\mathrm{m}} - \Gamma_{11}\Gamma_{11}^{\mathrm{m}}) & (\Gamma_{11}\Gamma_{21}^{\mathrm{m}} + \Gamma_{21}\Gamma_{11}^{\mathrm{m}}) \\ \Gamma_{21} & \Gamma_{11} & 0 & 1 & -(\Gamma_{11}\Gamma_{21}^{\mathrm{m}} + \Gamma_{21}\Gamma_{11}^{\mathrm{m}}) & (\Gamma_{21}\Gamma_{21}^{\mathrm{m}} - \Gamma_{11}\Gamma_{11}^{\mathrm{m}}) \\ \Gamma_{12} & -\Gamma_{22} & 1 & 0 & (\Gamma_{22}\Gamma_{22}^{\mathrm{m}} - \Gamma_{12}\Gamma_{12}^{\mathrm{m}}) & (\Gamma_{12}\Gamma_{22}^{\mathrm{m}} + \Gamma_{22}\Gamma_{12}^{\mathrm{m}}) \\ \Gamma_{22} & \Gamma_{12} & 0 & 1 & -(\Gamma_{12}\Gamma_{22}^{\mathrm{m}} + \Gamma_{22}\Gamma_{12}^{\mathrm{m}}) & (\Gamma_{22}\Gamma_{22}^{\mathrm{m}} - \Gamma_{12}\Gamma_{12}^{\mathrm{m}}) \\ \Gamma_{13} & -\Gamma_{23} & 1 & 0 & (\Gamma_{23}\Gamma_{23}^{\mathrm{m}} - \Gamma_{13}\Gamma_{13}^{\mathrm{m}}) & (\Gamma_{13}\Gamma_{23}^{\mathrm{m}} + \Gamma_{23}\Gamma_{13}^{\mathrm{m}}) \\ \Gamma_{23} & \Gamma_{13} & 0 & 1 & -(\Gamma_{13}\Gamma_{23}^{\mathrm{m}} + \Gamma_{23}\Gamma_{13}^{\mathrm{m}}) & (\Gamma_{23}\Gamma_{23}^{\mathrm{m}} - \Gamma_{13}\Gamma_{13}^{\mathrm{m}}) \end{bmatrix} \begin{bmatrix} A_1 \\ A_2 \\ B_1 \\ B_2 \\ C_1 \\ C_2 \end{bmatrix} = \begin{bmatrix} \Gamma_{11}^{\mathrm{m}} \\ \Gamma_{21}^{\mathrm{m}} \\ \Gamma_{12}^{\mathrm{m}} \\ \Gamma_{22}^{\mathrm{m}} \\ \Gamma_{13}^{\mathrm{m}} \\ \Gamma_{23}^{\mathrm{m}} \end{bmatrix} \tag{56}$$

The measurements and artifact values ($\boldsymbol{\Gamma}_i^{\mathrm{m}}$ and $\boldsymbol{\Gamma}_i$) are complex inputs to the calibration procedure with uncertain values. There is a total of twelve components associated with these quantities, which can be collected in a column vector

$$\begin{aligned} \mathbf{x} &= \begin{bmatrix} \boldsymbol{\Gamma}_1^{\mathrm{m}} & \boldsymbol{\Gamma}_1 & \boldsymbol{\Gamma}_2^{\mathrm{m}} & \boldsymbol{\Gamma}_2 & \boldsymbol{\Gamma}_3^{\mathrm{m}} & \boldsymbol{\Gamma}_3 \end{bmatrix}' \\ &\Leftrightarrow \begin{bmatrix} \Gamma_{11}^{\mathrm{m}} & \Gamma_{21}^{\mathrm{m}} & \Gamma_{11} & \Gamma_{21} & \Gamma_{12}^{\mathrm{m}} & \Gamma_{22}^{\mathrm{m}} & \Gamma_{12} & \Gamma_{22} & \Gamma_{13}^{\mathrm{m}} & \Gamma_{23}^{\mathrm{m}} & \Gamma_{13} & \Gamma_{23} \end{bmatrix}' , \end{aligned}$$

the 1-port calibration constants are the 'output' quantities

$$\begin{aligned} \mathbf{y} &= \begin{bmatrix} \boldsymbol{A} & \boldsymbol{B} & \boldsymbol{C} \end{bmatrix}' \\ &\Leftrightarrow \begin{bmatrix} A_1 & A_2 & B_1 & B_2 & C_1 & C_2 \end{bmatrix}' \end{aligned}$$

[8] The development in this section is based on [2] but is formally equivalent to [9].

and the measured values (a subset of the inputs) can be conveniently grouped as

$$\begin{aligned} \mathbf{t} &= \left[\begin{array}{ccc} \mathbf{\Gamma}_1^{\mathrm{m}} & \mathbf{\Gamma}_2^{\mathrm{m}} & \mathbf{\Gamma}_3^{\mathrm{m}} \end{array} \right]' \\ &\Leftrightarrow \left[\begin{array}{cccccc} \Gamma_{11}^{\mathrm{m}} & \Gamma_{21}^{\mathrm{m}} & \Gamma_{12}^{\mathrm{m}} & \Gamma_{22}^{\mathrm{m}} & \Gamma_{13}^{\mathrm{m}} & \Gamma_{23}^{\mathrm{m}} \end{array} \right]' . \end{aligned}$$

The implicit vector equation (55) can now be written

$$\mathbf{f}(\mathbf{x}, \mathbf{y}) = \mathbf{0} = \mathbf{H}(\mathbf{x})\, \mathbf{y} - \mathbf{t}(\mathbf{x}) , \tag{57}$$

where $\mathbf{H}(\mathbf{x})$ is the matrix on the left in (55).

The input covariance matrix, $\mathbf{V_x}$, is needed to obtain the output covariance matrix, as in (12). However, in this case the Jacobian matrix of the outputs with respect to the inputs, $\frac{\partial \mathbf{y}}{\partial \mathbf{x}'}$, is not immediately available, because $\mathbf{f}(\mathbf{x}, \mathbf{y})$ is implicit. Instead, the Jacobian can be found as the matrix product

$$\frac{\partial \mathbf{y}}{\partial \mathbf{x}'} = -\left(\frac{\partial \mathbf{f}}{\partial \mathbf{y}'} \right)^{-1} \frac{\partial \mathbf{f}}{\partial \mathbf{x}'} .$$

Differentiating (57) we obtain

$$\frac{\partial \mathbf{f}}{\partial \mathbf{x}'} = \left[\begin{array}{ccc} \frac{\partial \mathbf{H}}{\partial \mathbf{\Gamma}_1^{\mathrm{m}}} \mathbf{y} & \cdots & \frac{\partial \mathbf{H}}{\partial \mathbf{\Gamma}_3} \mathbf{y} \end{array} \right] - \left[\begin{array}{ccc} \frac{\partial \mathbf{t}}{\partial \mathbf{\Gamma}_1^{\mathrm{m}}} & \cdots & \frac{\partial \mathbf{t}}{\partial \mathbf{\Gamma}_3} \end{array} \right]$$

or in full scalar form

$$\frac{\partial \mathbf{f}}{\partial \mathbf{x}'} = \left[\begin{array}{ccc} \frac{\partial \mathbf{H}}{\partial \Gamma_{11}^{\mathrm{m}}} \mathbf{y} & \cdots & \frac{\partial \mathbf{H}}{\partial \Gamma_{23}} \mathbf{y} \end{array} \right] - \left[\begin{array}{ccc} \frac{\partial \mathbf{t}}{\partial \Gamma_{11}^{\mathrm{m}}} & \cdots & \frac{\partial \mathbf{t}}{\partial \Gamma_{23}} \end{array} \right]$$

and

$$\frac{\partial \mathbf{f}}{\partial \mathbf{y}'} = \mathbf{H}(\mathbf{x}) .$$

The Jacobian can therefore be found as the solution to

$$\mathbf{H}(\mathbf{x}) \frac{\partial \mathbf{y}}{\partial \mathbf{x}'} = \frac{\partial \mathbf{f}}{\partial \mathbf{x}'} , \tag{58}$$

for which conventional matrix algorithms can be used again.

5.1.1 Complex form of matrices

The $\frac{\partial \mathbf{H}}{\partial \boldsymbol{x}_i}$ matrices follow the pattern suggested by the first two:

$$\frac{\partial \mathbf{H}}{\partial \mathbf{\Gamma}_1^{\mathrm{m}}} = \left[\begin{array}{ccc} 0 & 0 & -\mathbf{\Gamma}_1 \\ 0 & 0 & 0 \\ 0 & 0 & 0 \end{array} \right] ,$$

and

$$\frac{\partial \mathbf{H}}{\partial \mathbf{\Gamma}_1} = \left[\begin{array}{ccc} 1 & 0 & -\mathbf{\Gamma}_1^{\mathrm{m}} \\ 0 & 0 & 0 \\ 0 & 0 & 0 \end{array} \right] .$$

The corresponding matrix products $\frac{\partial \mathbf{H}}{\partial \boldsymbol{x}_i} \mathbf{y}$ are:

$$\frac{\partial \mathbf{H}}{\partial \mathbf{\Gamma}_1^{\mathrm{m}}} \mathbf{y} = \left[\begin{array}{ccc} -\boldsymbol{C}\mathbf{\Gamma}_1 & 0 & 0 \end{array} \right]'$$

and

$$\frac{\partial \mathbf{H}}{\partial \Gamma_1} \mathbf{y} = \left[\begin{array}{ccc} \boldsymbol{A} - \boldsymbol{C}\mathbf{\Gamma}_1^{\mathrm{m}} & 0 & 0 \end{array} \right]' .$$

From these, the (3×4) complex matrix $\frac{\partial \mathbf{f}}{\partial \mathbf{x}'}$ can be constructed. It has a block-diagonal form

$$\begin{bmatrix} \mathbf{D}_1 & 0 & 0 \\ 0 & \mathbf{D}_2 & 0 \\ 0 & 0 & \mathbf{D}_3 \end{bmatrix},$$

where the diagonal blocks are the (2×1) complex matrices

$$\mathbf{D}_1 = \begin{bmatrix} -\boldsymbol{C}\boldsymbol{\Gamma}_1 - 1 \\ \boldsymbol{A} - \boldsymbol{C}\boldsymbol{\Gamma}_1^{\mathrm{m}} \end{bmatrix}',$$

$$\mathbf{D}_2 = \begin{bmatrix} -\boldsymbol{C}\boldsymbol{\Gamma}_2 - 1 \\ \boldsymbol{A} - \boldsymbol{C}\boldsymbol{\Gamma}_2^{\mathrm{m}} \end{bmatrix}'$$

and

$$\mathbf{D}_3 = \begin{bmatrix} -\boldsymbol{C}\boldsymbol{\Gamma}_3 - 1 \\ \boldsymbol{A} - \boldsymbol{C}\boldsymbol{\Gamma}_3^{\mathrm{m}} \end{bmatrix}'.$$

5.1.2 Scalar form of matrices

The twelve $\frac{\partial \mathbf{H}}{\partial x_i}$ matrices follow the pattern suggested by the first four:[9]

$$\frac{\partial \mathbf{H}}{\partial \Gamma_{11}^{\mathrm{m}}} = \begin{bmatrix} 0 & 0 & 0 & 0 & -\Gamma_{11} & \Gamma_{21} \\ 0 & 0 & 0 & 0 & -\Gamma_{21} & -\Gamma_{11} \\ 0 & 0 & 0 & 0 & 0 & 0 \\ 0 & 0 & 0 & 0 & 0 & 0 \\ 0 & 0 & 0 & 0 & 0 & 0 \end{bmatrix},$$

$$\frac{\partial \mathbf{H}}{\partial \Gamma_{21}^{\mathrm{m}}} = \begin{bmatrix} 0 & 0 & 0 & 0 & \Gamma_{21} & \Gamma_{11} \\ 0 & 0 & 0 & 0 & -\Gamma_{11} & \Gamma_{21} \\ 0 & 0 & 0 & 0 & 0 & 0 \\ 0 & 0 & 0 & 0 & 0 & 0 \\ 0 & 0 & 0 & 0 & 0 & 0 \end{bmatrix},$$

$$\frac{\partial \mathbf{H}}{\partial \Gamma_{11}} = \begin{bmatrix} 1 & 0 & 0 & 0 & -\Gamma_{11}^{\mathrm{m}} & \Gamma_{21}^{\mathrm{m}} \\ 0 & 1 & 0 & 0 & -\Gamma_{21}^{\mathrm{m}} & -\Gamma_{11}^{\mathrm{m}} \\ 0 & 0 & 0 & 0 & 0 & 0 \\ 0 & 0 & 0 & 0 & 0 & 0 \\ 0 & 0 & 0 & 0 & 0 & 0 \end{bmatrix},$$

$$\frac{\partial \mathbf{H}}{\partial \Gamma_{21}} = \begin{bmatrix} 0 & -1 & 0 & 0 & \Gamma_{21}^{\mathrm{m}} & \Gamma_{11}^{\mathrm{m}} \\ 1 & 0 & 0 & 0 & -\Gamma_{11}^{\mathrm{m}} & \Gamma_{21}^{\mathrm{m}} \\ 0 & 0 & 0 & 0 & 0 & 0 \\ 0 & 0 & 0 & 0 & 0 & 0 \\ 0 & 0 & 0 & 0 & 0 & 0 \end{bmatrix}.$$

The corresponding matrix products $\frac{\partial \mathbf{H}}{\partial x_i} \mathbf{y}$ are:

$$\frac{\partial \mathbf{H}}{\partial \Gamma_{11}^{\mathrm{m}}} \mathbf{y} = \begin{bmatrix} (-C_1\Gamma_{11} + C_2\Gamma_{21}) & -(C_1\Gamma_{21} + C_2\Gamma_{11}) & 0 & 0 & 0 & 0 \end{bmatrix}',$$

$$\frac{\partial \mathbf{H}}{\partial \Gamma_{21}^{\mathrm{m}}} \mathbf{y} = \begin{bmatrix} (C_1\Gamma_{21} + C_2\Gamma_{11}) & (-C_1\Gamma_{11} + C_2\Gamma_{21}) & 0 & 0 & 0 & 0 \end{bmatrix}',$$

$$\frac{\partial \mathbf{H}}{\partial \Gamma_{11}} \mathbf{y} = \begin{bmatrix} (A_1 - C_1\Gamma_{11}^{\mathrm{m}} + C_2\Gamma_{21}^{\mathrm{m}}) & (A_2 - C_1\Gamma_{21}^{\mathrm{m}} - C_2\Gamma_{11}^{\mathrm{m}}) & 0 & 0 & 0 & 0 \end{bmatrix}',$$

[9] This section was originally derived using the scalar forms of all equations. Clearly it can be obtained by simple transformation of the complex terms in the matrices of the previous section. Note that this is considerably easier: there are half the number of derivative matrices required and there are a quarter of the number of individual terms.

$$\frac{\partial \mathbf{H}}{\partial \Gamma_{21}} \mathbf{y} = \left[\begin{array}{cccccc} -(A_2 - C_1\Gamma^{\mathrm{m}}_{21} - C_2\Gamma^{\mathrm{m}}_{11}) & (A_1 - C_1\Gamma^{\mathrm{m}}_{11} + C_2\Gamma^{\mathrm{m}}_{21}) & 0 & 0 & 0 & 0 \end{array} \right]' .$$

From these, the (6×12) matrix $\frac{\partial \mathbf{f}}{\partial \mathbf{x}'}$ can be constructed. It has a block-diagonal form

$$\left[\begin{array}{ccc} \mathbf{D}_1 & 0 & 0 \\ 0 & \mathbf{D}_2 & 0 \\ 0 & 0 & \mathbf{D}_3 \end{array} \right] ,$$

where the diagonal blocks are the (2×4) matrices

$$\mathbf{D}_1 = \left[\begin{array}{cc} -C_1\Gamma_{11} + C_2\Gamma_{21} - 1 & -(C_1\Gamma_{21} + C_2\Gamma_{11}) \\ C_1\Gamma_{21} + C_2\Gamma_{11} & -C_1\Gamma_{11} + C_2\Gamma_{21} - 1 \\ A_1 - C_1\Gamma^{\mathrm{m}}_{11} + C_2\Gamma^{\mathrm{m}}_{21} & A_2 - C_1\Gamma^{\mathrm{m}}_{21} - C_2\Gamma^{\mathrm{m}}_{11}) \\ -(A_2 - C_1\Gamma^{\mathrm{m}}_{21} - C_2\Gamma^{\mathrm{m}}_{11}) & A_1 - C_1\Gamma^{\mathrm{m}}_{11} + C_2\Gamma^{\mathrm{m}}_{21} \end{array} \right]' ,$$

$$\mathbf{D}_2 = \left[\begin{array}{cc} -C_1\Gamma_{12} + C_2\Gamma_{22} - 1 & -(C_1\Gamma_{22} + C_2\Gamma_{12}) \\ C_1\Gamma_{22} + C_2\Gamma_{12} & -C_1\Gamma_{12} + C_2\Gamma_{22} - 1 \\ A_1 - C_1\Gamma^{\mathrm{m}}_{12} + C_2\Gamma^{\mathrm{m}}_{22}) & A_2 - C_1\Gamma^{\mathrm{m}}_{22} - C_2\Gamma^{\mathrm{m}}_{12}) \\ -(A_2 - C_1\Gamma^{\mathrm{m}}_{22} - C_2\Gamma^{\mathrm{m}}_{12}) & A_1 + C_1\Gamma^{\mathrm{m}}_{12} + C_2\Gamma^{\mathrm{m}}_{22} \end{array} \right]'$$

and

$$\mathbf{D}_3 = \left[\begin{array}{cc} -C_1\Gamma_{13} + C_2\Gamma_{23} - 1 & -(C_1\Gamma_{23} + C_2\Gamma_{13}) \\ C_1\Gamma_{23} + C_2\Gamma_{13} & -C_1\Gamma_{13} + C_2\Gamma_{23} - 1 \\ A_1 - C_1\Gamma^{\mathrm{m}}_{13} + C_2\Gamma^{\mathrm{m}}_{23} & A_2 - C_1\Gamma^{\mathrm{m}}_{23} - C_2\Gamma^{\mathrm{m}}_{13} \\ -(A_2 - C_1\Gamma^{\mathrm{m}}_{23} - C_2\Gamma^{\mathrm{m}}_{13}) & A_1 - C_1\Gamma^{\mathrm{m}}_{13} + C_2\Gamma^{\mathrm{m}}_{23} \end{array} \right]' .$$

5.2 Two-port uncertainty

Six error terms remain, involving signal flow between the two measurement ports of the VNA.

The uncertainty of the two leakage terms is straightforward, because it is equal to the measurement uncertainties of S^{m}_{21} and S^{m}_{12}.

The four remaining terms, equations (32) – (35), are more laborious to calculate. For example, the forward load match, $E^{\mathrm{F}}_{\mathrm{L}}$ (32), is an explicit function of eight uncertain complex quantities (S^{m}_{11}, A^{F}, B^{F}, C^{F}, S_{11}, S_{12}, S_{21} and S_{22}). So a (16×16) covariance matrix describes the input uncertainties and a (2×16) Jacobian matrix is needed to obtain the covariance of the error term. Similarly, the forward tracking, $E^{\mathrm{F}}_{\mathrm{T}}$, is a function of nine complex inputs!

Nonetheless, the techniques described in Section 3.1 apply to these cases and can be used to obtain the covariance of the remaining error terms.

6 Application

To show how the theory of the previous sections can be applied, this section carries out the calculations for a VNA calibration for measurements of reflection coefficients. This is a one-port calibration exercise (see Section 5.1).

Three calibration standards must be measured using the VNA: a short, a matched (50 ohm) load, and an open. Ordinarily, the estimated values and uncertainties of these artifacts would be known. This information provides the traceability to national standards of subsequent VNA measurements (once the VNA is calibrated). In this example, we simply assume ideal values for the three artifacts ($\Gamma = -1$, $\Gamma = 0$ and $\Gamma = 1$ for the short, load and open respectively) and attribute uncertainties of 0.01 to both real and imaginary components in each case (with no correlation). This choice of uncertainty value is compatible, if a little pessimistic, with the stated capabilities of several national laboratories on the current BPIM Key comparison database.

Measurements of these three types of calibration artifacts were made on our VNA (Agilent 8753ES) at a frequency of 1 GHz. The results are presented in Table 1. The uncertainties in these values were taken to be 0.01 in both the real and imaginary components (with no correlation), which is compatible with European guidelines [11] (the arbitrary choice is only for the purpose of the example).

label	artifact	real	imaginary
A	short	-0.188	-0.902
B	load	0.006	0.007
C	open	0.239	0.936

Table 1: Measured values of the reflection coefficient (S_{11}) for three calibration artifacts. The label in the first column maps the artifact to one of the variables referred to in Section 5.1 (this assignment is arbitrary).

To carry out the uncertainty calculations, the matrices in Section 5.1 were assembled. In particular,

$$\mathbf{H} = \begin{bmatrix} -1 & 0 & 1 & 0 & -0.188 & 0.902 \\ 0 & -1 & 0 & 1 & -0.902 & -0.188 \\ 1 & 0 & 1 & 0 & -0.239 & 0.936 \\ 0 & 1 & 0 & 1 & -0.936 & -0.239 \\ 0 & 0 & 1 & 0 & 0 & 0 \\ 0 & 0 & 0 & 1 & 0 & 0 \end{bmatrix}$$

Equation (57) was solved, using LU decomposition, to obtain the solution vector

$$\mathbf{y} = \begin{bmatrix} 0.212816 & 0.919197 & 0.006 & 0.007 & -0.0150012 & 0.0177337 \end{bmatrix}' .$$

The components of this vector are the complex values of A, B and C:
$A = 0.212816 + j\,0.919197$, $B = 0.006 + j\,0.007$ and $C = -0.0150012 + j\,0.0177337$.

With these values for the components of $\mathbf{y}$, the Jacobian matrix $\frac{\partial \mathbf{f}}{\partial \mathbf{x}'}$ is

$$\begin{bmatrix} -0.01015 & 0.000177337 & 0 & 0 & 0 & 0 \\ -0.000177337 & -0.01015 & 0 & 0 & 0 & 0 \\ 0.00194 & 0.00909 & 0 & 0 & 0 & 0 \\ -0.00909 & 0.00194 & 0 & 0 & 0 & 0 \\ 0 & 0 & -0.00984999 & -0.000177337 & 0 & 0 \\ 0 & 0 & 0.000177337 & -0.00984999 & 0 & 0 \\ 0 & 0 & 0.00233 & 0.00929 & 0 & 0 \\ 0 & 0 & -0.00929 & 0.00233 & 0 & 0 \\ 0 & 0 & 0 & 0 & -0.01 & 0 \\ 0 & 0 & 0 & 0 & 0 & -0.01 \\ 0 & 0 & 0 & 0 & 0.0021303 & 0.00919196 \\ 0 & 0 & 0 & 0 & -0.00919196 & 0.0021303 \end{bmatrix}'$$

Equation (58) can be solved and the variance-covariance matrix for the estimates $\mathbf{y}$ can be obtained. This matrix is

$$\begin{bmatrix} 9.48652e-05 & 0.0 & 4.47383e-06 & 4.20578e-06 & 8.16351e-06 & -5.58613e-06 \\ 0.0 & 9.48652e-05 & -4.20578e-06 & 4.47383e-06 & 5.58613e-06 & 8.16351e-06 \\ 4.47383e-06 & -4.20578e-06 & 1.89030e-04 & 0.0 & 4.53387e-05 & -1.95158e-04 \\ 4.20578e-06 & 4.47383e-06 & 0.0 & 1.890303e-04 & 1.95158e-04 & 4.53387e-05 \\ 8.163501e-06 & 5.58613e-06 & 4.53387e-05 & 1.95158e-04 & 3.18587e-04 & 0.0 \\ -5.58613e-06 & 8.16351e-06 & -1.95158e-04 & 4.53387e-05 & 0.0 & 3.18587e-04 \end{bmatrix}$$

entries less than 10^{-20} are displayed as zero, to allow for numerical round-off in the calculation.

Finally, values and uncertainties for the three one-port error terms can be obtained. The directivity, $E_{\mathrm{D}} = B = 0.006 + j\,0.007$. The uncertainty in this estimate is described by a simple diagonal variance-covariance matrix with equal diagonal elements: 1.9×10^{-4}. The source match, $E_{\mathrm{S}} = -C = 0.0150 - j\,0.0177$ with a diagonal variance-covariance matrix with equal diagonal elements: 3.2×10^{-4}. Finally, the reflection tracking, $E_{\mathrm{R}} = A - BC = 0.2130 + j\,0.9192$. Again the covariance matrix is diagonal with equal elements: 9.5×10^{-5}.

7 Discussion

This report has described the mathematics involved in calculating and propagating uncertainties when using a vector network analyser. Clearly, manipulation of the equations by hand is laborious, so there is a need to automate calculations. Indeed, it is reasonable to assume that adoption of techniques described above would have already occurred, were it not for the lack of convenient tools to perform the calculations. Work has already begun on suitable techniques, which will be reported on in the future.

It must be borne in mind that the technique of uncertainty propagation described is based on two key assumptions. First, the uncertainty in a complex parameter can be adequately modeled by a bivariate Gaussian distribution. Second, the calculations use a linear approximation to the form of measurement equations in the vicinity of the estimated value. This could lead to unreasonable uncertainty statements if estimates lie close to local turning points in the measurement function. To address this, the sensitivity of uncertainty results to a particular set of estimated values should be investigated. This could be done by varying values, or alternatively a Monte Carlo calculation could validate the method when applied in a particular type of problem.

References

[1] *Guide to the Expression of Uncertainty in Measurement* (Geneva: International Organization for Standardization, 1995)

[2] K. Weise, IEEE Trans. Instrum. Meas. **IM-36**(2) (1987) pp 642-645

[3] J. Fitzpatrick, Microwave Journal **May** (1978) pp 63-66.

[4] D. Woods, Electron. Lett. **11**(17) (1975) pp 403-404.

[5] D. C. DeGroot, K. L. Reed, and J. A. Jargon, 54th ARFTG Conf. Dig. (1999) pp 103-115.

[6] D. Kostevc and J. Mlakar Microwave Journal **July** (2000) pp 88-94.

[7] D. M. Kerns and R. W. Beatty, *Basic theory of waveguide junctions and introductory microwave network analysis* (Pergamon, Oxford, 1967).

[8] R. B. Marks, 50th ARFTG Conf. Dig. (1997) pp 115-126.

[9] M. G. Cox, M. P. Daiton, P. M. Harris, N. M. Ridler and P. R. Young, *A generalised treatment of the uncertainty in calibration and measurement of vector indicating microwave reflectormeters*, NPL Report

[10] M. R. Spiegel, *Complex Variables* (Schaum's Outline Series, McGraw-Hill, Great Britain, 1974)

[11] *EA guidelines on the evaluation of vector network analysers* (European Co-operation for Accreditation) **EA-10**/12 May 2000.